Depth-Dependent Solvent Relaxation in Reverse Micelles: A Fluorescence Approach

Devaki A. Kelkar and Amitabha Chattopadhyay*

Centre for Cellular and Molecular Biology, Uppal Road, Hyderabad 500 007, India

Received: March 27, 2004; In Final Form: June 4, 2004

We report here depth-dependent solvent relaxation effects in the reverse micellar assembly using the deeply embedded probe NBD-cholesterol, a fluorescent cholesterol analogue in which the 7-nitrobenz-2-oxa-1,3-diazol-4-yl (NBD) group is covalently attached to the flexible acyl chain of cholesterol. Because of its deeper location, the NBD group of NBD-cholesterol is capable of reporting solvation dynamics in the deeper regions of the organized molecular assembly in which it is incorporated. NBD-cholesterol exhibits red edge excitation shift (REES) when incorporated into reverse micelles formed by sodium bis(2-ethylhexyl) sulfosuccinate (AOT) in isooctane with varying [water]/[surfactant] molar ratio (w_o). Interestingly, the extent of REES increases with increasing w_o implying that the overall motional restriction experienced by the reorienting solvent molecules is increased with increasing hydration. This is in contrast to the behavior of interfacially localized probes. In addition, our results show that with increasing w_o, the NBD group of NBD-cholesterol experiences increased polarity as evidenced by the decrease in fluorescence lifetime and other fluorescence parameters such as fluorescence intensity. NBD-cholesterol could prove to be a useful probe for monitoring depth-dependent dynamics in organized molecular assemblies.

Introduction

Amphiphilic surfactants self-assemble to form reverse (or inverted) micelles in nonpolar solvents in which the polar headgroups of the surfactant monomers cluster to form a micellar core and are directed toward the center of the assembly and the hydrophobic tails extend outward into the bulk organic phase.[1,2] Reverse micelles are relatively simple yet versatile systems and represent a unique type of self-organized molecular assembly. They provide an attractive model system for biomembranes since they mimic several important and essential features of biological membranes although lacking much of the complexity associated with them. The general principles underlying the formation of reverse micelles are common to other related assemblies such as micelles, bilayers, liposomes, and membranes.[3−6] The highly structured yet heterogeneous water molecules in reverse micelles represent interesting models for water molecules present in biological systems such as membranes, which are more difficult to analyze experimentally. The physical and chemical properties of the entrapped water are markedly different from the properties of bulk water but similar in several aspects to those of biological interfacial water as found in membranes or protein interfaces.[7−10] The interfacial water is crucial for the induction of secondary structure in peptides and proteins when bound to surfaces such as membranes or micelles as well as for variation of their local internal motion. Both experimental[7−9] and theoretical[11] approaches have shown that the key structural parameter of reverse micelles is the [water]/[surfactant] molar ratio (w_o), which determines the micellar size as well as the unique physicochemical properties of the entrapped water. Reverse micelles therefore represent a type of organized molecular assembly that offers the unique advantage of monitoring dynamics of embedded molecules with varying degrees of hydration. A wide range of physicochemical properties of the micellar water such as micropolarity, dielectric constant, microviscosity, water activity, freezing point, proton-transfer efficiency, and the hydrogen-bonding potential of the aqueous inner core can be experimentally varied with w_o, providing a unique and versatile reaction medium.

The double chain anionic surfactant AOT (sodium bis(2-ethylhexyl) sulfosuccinate) has been extensively used to form reverse micelles in nonpolar solvents. One of the advantages for using AOT is that reverse micelles formed by AOT can solubilize a large quantity of water in a nonpolar solvent. In addition, reverse micelles formed by AOT retain a spherical shape over a wide range of w_o. As a result of this, the radius of the entrapped water pool can be linearly related to w_o.[12,13]

Fluorescence techniques have been widely used to characterize reverse micellar organization and dynamics because of its intrinsic sensitivity, suitable time resolution, minimal perturbation, and noninvasive nature.[14−16] Reverse micelles offer certain inherent advantages in fluorescence studies since they are small and optically transparent, have well-defined sizes, and are relatively scatter-free. They are highly cooperative, organized molecular assemblies of amphiphilic surfactants, and are dynamic in nature. A direct consequence of such organized systems is the restriction imposed on the dynamics and mobility of their constituent structural units. We have previously shown that the microenvironment of molecules bound to such organized assemblies can be conveniently monitored using wavelength-selective fluorescence as a novel tool.[15−27] Wavelength-selective fluorescence comprises a set of approaches based on the red edge effect in fluorescence spectroscopy which can be used to directly monitor the environment and dynamics around a fluorophore in an organized molecular assembly.[28−31] A shift in the wavelength of maximum fluorescence emission toward higher wavelengths, caused by a shift in the excitation wavelength toward the red edge of absorption band, is termed red

* Address correspondence to this author. Telephone: +91-40-2719-2578; fax: +91-40-2716-0311; e-mail: amit@ccmb.res.in.

10.1021/jp048645z CCC: $27.50
Published on Web 07/13/2004

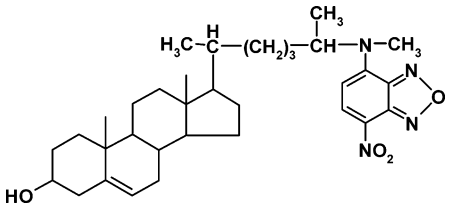

Figure 1. Chemical structure of NBD-cholesterol.

edge excitation shift (REES).[28−33] This effect is mostly observed with polar fluorophores in motionally restricted environments such as viscous solutions or condensed phases where the dipolar relaxation time for the solvent shell around a fluorophore is comparable to or longer than its fluorescence lifetime.[28−35] REES arises because of slow rates of solvent relaxation (reorientation) around an excited state fluorophore, which is dependent on the motional restriction imposed on the solvent molecules in the immediate vicinity of the fluorophore. Utilizing this approach, it becomes possible to probe the mobility parameters of the environment itself (which is represented by the relaxing solvent molecules) using the fluorophore merely as a reporter group. This makes the use of REES in particular and the wavelength-selective fluorescence approach in general very useful since hydration plays a crucial modulatory role in the formation and maintenance of organized molecular assemblies such as micelles, membranes, and folded proteins in aqueous solutions.[36]

NBD (7-nitrobenz-2-oxa-1,3-diazol-4-yl)-labeled lipids are widely used as fluorescent analogues of native lipids in biological and model membranes and membrane−mimetic systems to study a variety of processes.[37] We have recently reported that the fluorescent lipid probe *N*-(7-nitrobenz-2-oxa-1,3-diazol-4-yl)-1,2-dipalmitoyl-*sn*-glycero-3-phosphoethan olamine (NBD-PE), in which the NBD group is covalently attached to the headgroup of phosphatidylethanolamine, when incorporated in reverse micelles of AOT, exhibits hydration-dependent REES and the extent of REES decreases with increasing w_o.[15] In this paper, we report the observation of red edge excitation shift of 25-[*N*-[(7-nitrobenz-2-oxa-1,3-diazol-4-yl)-methyl]amino]-27-norcholesterol (NBD-cholesterol) when incorporated into AOT reverse micelles. In contrast to NBD-PE, the NBD group in NBD-cholesterol is covalently attached to the flexible acyl chain of the cholesterol molecule (see Figure 1). The NBD group of this molecule is localized in the hydrocarbon region of the membrane[38−41] and membrane−mimetic media such as micelles.[22] Because of its deeper location, the NBD group of NBD-cholesterol is capable of reporting solvation dynamics in the deeper regions of the organized molecular assembly in which it is incorporated. This is important since unlike bulk solvents, these compartmentalized molecular assemblies are anisotropic in nature and therefore display differential solvent relaxation rates in different regions of the assembly. In an earlier work, we used the spatial localization of NBD-cholesterol in the membrane bilayer to monitor water penetration in the deeper hydrocarbon region of the membrane.[23]

Reverse micelles represent a type of organized molecular assembly which offer the unique advantage of monitoring dynamics of molecules with varying states of hydration. Application of the wavelength-selective fluorescence approach to reverse micellar systems is therefore particularly appealing since REES is capable of monitoring the dynamics of the solvent molecules surrounding the fluorophore. We report here, that unlike the shallow interfacial probe NBD-PE, REES of NBD-cholesterol in AOT reverse micelles increases with increasing hydration (w_o) of the reverse micelle. This implies that the rate of solvent relaxation changes with change in probe location in reverse micelles, as shown earlier in membranes using anthroyloxy fatty acid probes.[21] This is supported by fluorescence polarization and lifetime data and the variation of these parameters with excitation wavelength.

Experimental Section

Materials. AOT was purchased from Sigma Chemical Co. (St. Louis. MO). NBD-cholesterol was from Avanti Polar Lipids (Alabaster, AL). 2-, 6-, and 12-(9-anthroyloxy)stearic acid (2-, 6-, and 12-AS) were from Molecular Probes (Eugene, OR). Water was purified through a Millipore (Bedford, MA) Milli-Q system and used throughout. The isooctane used was of spectroscopic grade. The purity of AOT was confirmed by good agreement of its UV absorption spectrum with previously reported spectrum.[1] The purity of NBD-cholesterol was checked by thin-layer chromatography on silica gel precoated plates (Sigma) in chloroform/methanol/water (65:35:4, v/v/v) and was pure when detected by its color or fluorescence.[40] Concentration of stock solutions of NBD-cholesterol in methanol were estimated using the molar absorption coefficient (ϵ) of 22 000 M^{-1} cm^{-1} at 484 nm.[23] Concentrations of stock solutions of 2-, 6-, and 12-AS in methanol were estimated as described earlier.[24]

Preparation of Reverse Micelles. Reverse micelles of AOT containing NBD-cholesterol (or 2-, 6-, or 12-AS) were prepared without the addition of any cosolvent as described earlier.[15] Briefly, NBD-cholesterol (or the AS probe) in methanol (12 nmol) was dried under a stream of nitrogen while being warmed gently (∼35 °C). After further drying under a high vacuum for at least 4 h, 1.5 mL of 50 mM AOT in isooctane was added, and samples were vortexed for 3 min. The samples were kept in the dark for an hour with intermittent vortexing (10 s of vortexing at intervals of 10 min) to incorporate the fluorescent probe into the reverse micelles and to obtain optically clear dispersions. Appropriate amounts of water were subsequently added to make reverse micellar dispersions of different [water]/[surfactant] molar ratios (w_o). The optical density of the fluorescent samples at the excitation wavelength was low (generally <0.18) in all cases. Background samples were prepared the same way except that fluorophore was not added to them. All experiments were done at 23 °C.

The molar ratio of fluorophore to surfactant was carefully chosen to give an optimum signal-to-noise ratio with minimal perturbation to the micellar organization and negligible interprobe interactions. The final fluorophore concentration was 8 μM while the concentration of AOT was 50 mM in all cases. This corresponds to a final molar ratio of fluorophore to surfactant of 1:6250 (mol/mol). At such a low fluorophore to surfactant molar ratio, not more than one probe molecule would be present per reverse micelle on an average, which rules out any probe aggregation effects, especially keeping in mind the aggregation number of AOT of ∼50−300 in the range of w_o between 5 and 25.[42]

Steady-State Fluorescence Measurements. Steady-state fluorescence measurements were performed with a Hitachi F-4010 spectrofluorometer using 1 cm path length quartz cuvettes. Excitation and emission slits with a nominal bandpass of 5 nm were used for all measurements. Background intensities of samples in which the fluorophore was omitted were negligible in most cases and were subtracted from each sample spectrum to cancel out any contribution due to the solvent Raman peak and other scattering artifacts. The spectral shifts obtained with different sets of samples were identical in most

cases. In other cases, the values were within ±1 nm of the ones reported. Fluorescence polarization measurements were performed using a Hitachi polarization accessory. Polarization values were calculated from the equation:[43]

$$P = \frac{I_{VV} - GI_{VH}}{I_{VV} + GI_{VH}} \quad (1)$$

where I_{VV} and I_{VH} are the measured fluorescence intensities (after appropriate background subtraction) with the excitation polarizer vertically oriented and emission polarizer vertically and horizontally oriented, respectively. G is the grating correction factor and is the ratio of the efficiencies of the detection system for vertically and horizontally polarized light and is equal to I_{HV}/I_{HH}. All experiments were done with multiple sets of samples and average values of polarization are shown in Figure 6.

Time-Resolved Fluorescence Measurements. Fluorescence lifetimes were calculated from time-resolved fluorescence intensity decays using a Photon Technology International (London, Western Ontario, Canada) LS-100 luminescence spectrophotometer in the time-correlated single-photon-counting mode. This machine uses a thyratron-gated nanosecond flash lamp filled with nitrogen as the plasma gas (17 ± 1 in. of mercury vacuum) and is run at 17−20 kHz. Lamp profiles were measured at the excitation wavelength using Ludox (colloidal silica) as the scatterer. To optimize the signal-to-noise ratio, 10 000 photon counts were collected in the peak channel. The excitation wavelength used was 465 nm and emission was set at 513 nm. All experiments were performed using excitation and emission slits with a nominal band-pass of 10 nm or less. The sample and the scatterer were alternated after every 5% acquisition to ensure compensation for shape and timing drifts occurring during the period of data collection. This arrangement also prevents any prolonged exposure of the sample to the excitation beam thereby avoiding any possible photodamage to the fluorophore. The data stored in a multichannel analyzer was routinely transferred to an IBM PC for analysis. Fluorescence intensity decay curves so obtained were deconvoluted with the instrument response function and analyzed as a sum of exponential terms:

$$F(t) = \sum_i \alpha_i \exp(-t/\tau_i) \quad (2)$$

where $F(t)$ is the fluorescence intensity at time t and α_i is a preexponential factor representing the fractional contribution to the time-resolved decay of the component with a lifetime τ_i such that $\Sigma_i \alpha_i = 1$. The decay parameters were recovered using a nonlinear least squares iterative fitting procedure based on the Marquardt algorithm.[44] The program also includes statistical and plotting subroutine packages.[45] The goodness of the fit of a given set of observed data and the chosen function was evaluated by the reduced χ^2 ratio, the weighted residuals,[46] and the autocorrelation function of the weighted residuals.[47] A fit was considered acceptable when plots of the weighted residuals and the autocorrelation function showed random deviation about zero with a minimum χ^2 value not more than 1.5. Mean (average) lifetimes $\langle\tau\rangle$ for biexponential decays of fluorescence were calculated from the decay times and preexponential factors using the following equation:[43]

$$\langle\tau\rangle = \frac{\alpha_1\tau_1^2 + \alpha_2\tau_2^2}{\alpha_1\tau_1 + \alpha_2\tau_2} \quad (3)$$

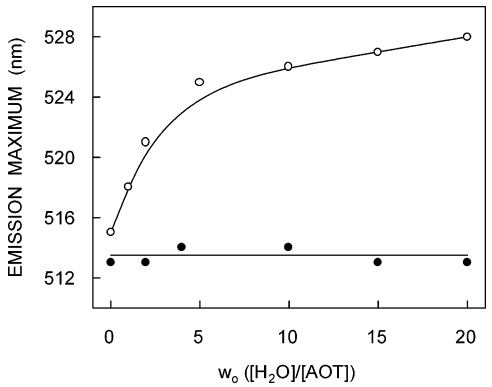

Figure 2. Effect of increasing amounts of added water on the wavelength of maximum emission of NBD-cholesterol (●) and NBD-PE (○) in AOT reverse micelles. The excitation wavelength used was 475 nm for NBD-cholesterol and 465 nm for NBD-PE. The data for NBD-PE is plotted from Figure 2 and Table 1 of ref 15. The ratio of fluorophore (NBD-labeled lipid) to surfactant (AOT) was 1:6250 (mol/mol) in both cases. See Experimental Section for other details.

Results

The Region of Localization of the NBD group of NBD-Cholesterol in Reverse Micelles Is Characterized by Unique Polarity Features. The fluorescence emission maxima of NBD-cholesterol in AOT reverse micelles as a function of increasing [water]/[surfactant] molar ratio (w_o) are shown in Figure 2. The maximum of fluorescence emission of NBD-cholesterol in the reverse micellar environment is at 513 nm. The emission maximum of NBD-cholesterol in model membranes of dioleoyl-*sn*-glycero-3-phosphocholine (DOPC) has earlier been reported by us to be 522 nm.[39] The relatively blue shifted emission maximum in reverse micelles indicates the nonpolar nature of the site of localization of the NBD group of NBD-cholesterol in the reverse micellar assembly. We have earlier shown that for NBD-labeled lipids incorporated in an organized molecular assembly such as membranes, the position of the emission maximum of the NBD group provides an overall indication of the polarity of the environment in which it is placed.[38,39] On the basis of such a correlation, it was estimated that an emission maximum of 513 nm would correspond to an environmental dielectric constant of ~4,[39] similar to what has been estimated as the dielectric constant experienced in reverse micelles.[48] Interestingly, Figure 2 shows that the emission maximum of NBD-cholesterol remains invariant over a large range of w_o (from 0 to 20).

In sharp contrast to the invariance of the emission maximum of NBD-cholesterol over a large range of w_o, the emission maximum of NBD-PE in AOT reverse micelles displays a progressive red shift of 13 nm (from 515 to 528 nm) over the same range of w_o. In NBD-PE, the NBD group is covalently attached to the headgroup of a phosphatidylethanolamine molecule and has earlier been shown to be localized in the interfacial region in membranes,[38,39,49−51] micelles,[19] and reverse micelles.[15] The lack of dependence of the emission maximum of NBD-cholesterol on w_o indicates that the NBD moiety of NBD-cholesterol is located in a deep region of the reverse micelle which is characterized by reduced water penetration.

The above results bring out the important point that increasing w_o in an organized anisotropic molecular assembly such as a reverse micelle does not necessarily imply uniform polarity shifts in all regions of the reverse micelle. In other words, the change in polarity experienced in an anisotropic assembly will be dependent on the position (location) of the incorporated probe. To explore this issue further, we designed experiments using

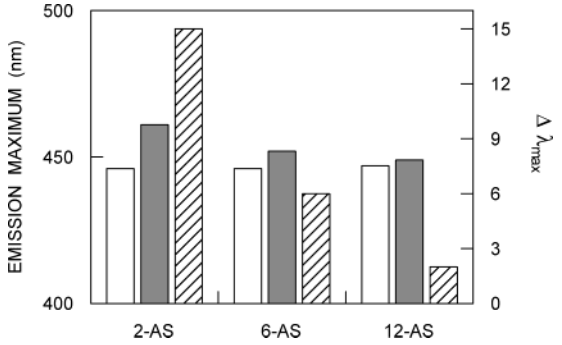

Figure 3. Effect of added water on the wavelength of maximum emission of 2-, 6-, and 12-AS in AOT reverse micelles. The open bars denote emission maximum recorded at $w_o = 0$ and the shaded bars correspond to $w_o = 25$. The hatched bars represent the difference in emission maximum ($\Delta\lambda_{max}$) in these two cases. The excitation wavelength used was 365 nm in all cases. The ratio of fluorophore (AS probe) to surfactant (AOT) was 1:6250 (mol/mol) in all cases. See Experimental Section for other details.

the well-known series of anthroyloxy fatty acid probes. The anthroyloxy fatty acids in which an anthracene group is attached by an ester linkage to various positions of an alkyl chain have been extensively used as fluorescent probes of micellar and bilayer structure.[21,52,53] These anthroyloxy fatty acids are well suited to probe such position-dependent effects since they locate at a graded series of depths in the bilayer. In fact, it has been shown that the depth of the anthroyloxy group in an organized assembly such as a bilayer is almost linearly related to the number of carbon atoms between it and the carboxyl group.[52]

Figure 3 shows the effect of added water (w_o) on the wavelength of maximum emission of the AS probes in AOT reverse micelles. As the figure shows, the fluorescence emission maximum of the shallow interfacial probe 2-AS is extremely sensitive to a change in w_o from 0 to 25 which is accompanied by a red shift of the emission maximum by 15 nm (see hatched bar in the figure). The sensitivity of the emission maximum of the anthroyloxy probes, however, reduces as the position (location) of the fluorophore (the anthroyloxy group) increases from the water pool. Thus, the red shift in emission maximum of 6- and 12-AS upon changing w_o from 0 to 25 is reduced to 6 and 2 nm, respectively. The sensitivity of the emission maximum to added water therefore appears to be dependent on the position of the fluorophore in the reverse micelle and decreases with increasing distance of the fluorophore from the water pool, that is, 2-AS > 6-AS > 12-AS. On the basis of this result and the invariance of the emission maximum of NBD-cholesterol to w_o (see Figure 2), the NBD group of NBD-cholesterol would be expected to be localized in the deeper region of the reverse micelle. Further results show that this region of localization is characterized by rates of solvent relaxation that are different from what is experienced at the interfacial region (see later).

The fluorescence emission spectra and intensity of NBD-cholesterol incorporated in AOT reverse micelles as a function of w_o are shown in Figure 4. Figure 4a shows that while there is no shift in the fluorescence emission maximum (as seen in Figure 2), the peak fluorescence intensity shows a progressive reduction with increasing w_o. The decrease in peak fluorescence intensity is ~52% when w_o is increased from 0 to 25 (see Figure 4b). The quantum yield of NBD fluorescence depends on the polarity of the medium in which the probe is located and is reduced in polar environments.[54,55] The decrease in fluorescence intensity may be attributed to the increased polarity around the NBD group with increasing water content of the reverse micelle.

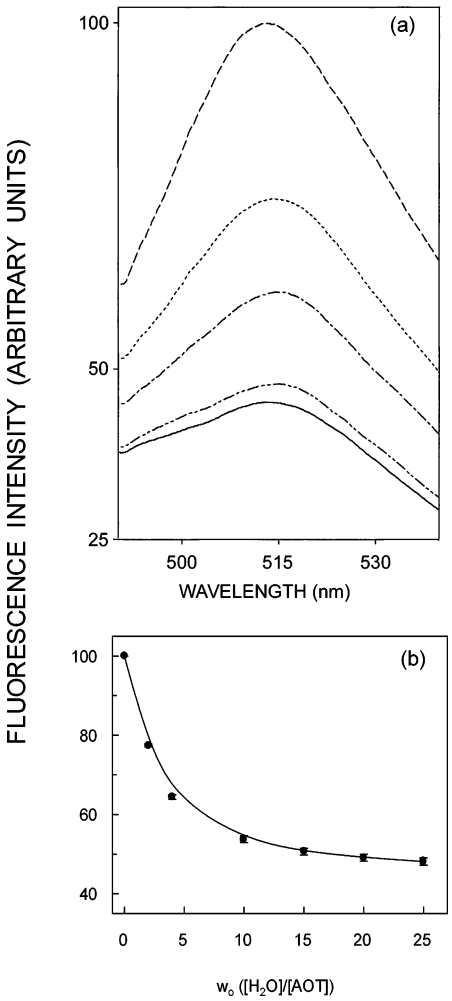

Figure 4. Effect of increasing amounts of added water on (a) fluorescence emission spectra and (b) fluorescence intensity of NBD-cholesterol in AOT reverse micelles. Fluorescence emission spectra are shown in (a) as a function of [water]/[surfactant] molar ratio (w_o) in order of decreasing intensity corresponding to $w_o = 0$ (---), 2 (···), 4 (-·-), 15 (-···-), and 25 (—). Fluorescence intensity was monitored at 513 nm and is plotted as a function of w_o in (b). The data points shown are the means ± standard errors of five independent measurements. The excitation wavelength used was 475 nm. The ratio of fluorophore (NBD-cholesterol) to surfactant (AOT) was 1:6250 (mol/mol) in all cases. See Experimental Section for other details.

Interestingly, Figure 4a also shows that with increasing w_o the reduction in fluorescence intensity is accompanied by spectral broadening. Such spectral broadening may be due to increased heterogeneity of the NBD solvation shell with increasing hydration of the reverse micelle, a situation encountered when the rate of solvent reorientation in the excited state is comparable to the fluorescence lifetime.[28]

Red Edge Excitation Shift of NBD-Cholesterol in Reverse Micelles of Varying Hydration. The shifts in the maxima of fluorescence emission[56] of NBD-cholesterol in AOT reverse micelles as a function of excitation wavelength are shown in Figure 5a. As the excitation wavelength is changed from 475 to 510 nm the emission maxima of NBD-cholesterol bound to AOT reverse micelles of varying w_o display shifts toward longer wavelengths in all cases. The emission maxima are shifted from 513 to 519 nm (for $w_o = 0$), 513 to 520 nm ($w_o = 2$), 514 to 522 nm ($w_o = 4$), and 513 to 524 ($w_o = 25$), which correspond to REES of 6−11 nm in these cases. It is possible that there could be further red shift when NBD-cholesterol is excited

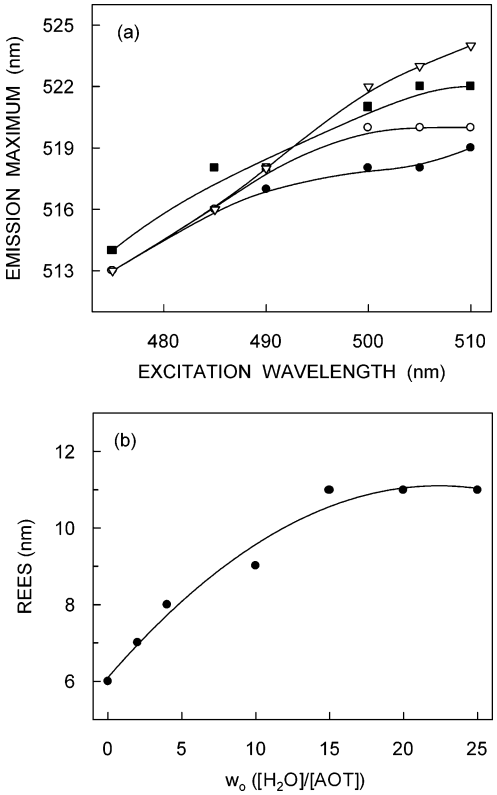

Figure 5. (a) Effect of changing excitation wavelength on the wavelength of maximum emission of NBD-cholesterol in AOT reverse micelles corresponding to $w_o = 0$ (●), 2 (○), 4 (■), and 25 (▽). (b) Effect of increasing amounts of water on the magnitude of REES of NBD-cholesterol in AOT reverse micelles. REES data obtained as in (a) is plotted as a function of [water]/[surfactant] molar ratio (w_o). All other conditions are as in Figure 4. See Experimental Section for other details.

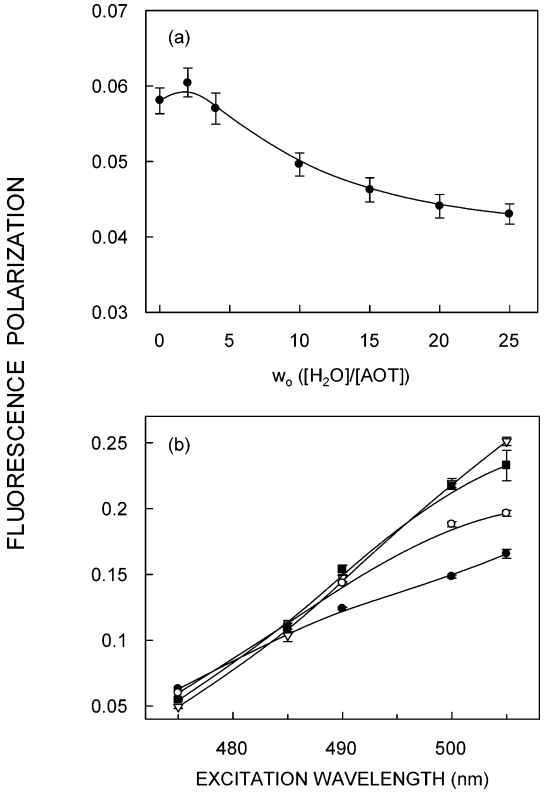

Figure 6. (a) Effect of increasing hydration on the fluorescence polarization of NBD-cholesterol in AOT reverse micelles. Polarization values were recorded at 513 nm and the excitation wavelength used was 475 nm. (b) Fluorescence polarization of NBD-cholesterol in AOT reverse micelles corresponding to $w_o = 0$ (●), 2 (○), 10 (■), and 25 (▽) as a function of excitation wavelength. The emission wavelength was 513 nm in all cases. The data points shown are the means ± standard errors of at least three independent measurements. All other conditions are as in Figure 4. See Experimental Section for other details.

beyond 510 nm. We found it difficult to work in this wavelength range because of low signal-to-noise ratio and scattering artifacts that sometimes remained even after background subtraction. Such dependence of the emission maximum on the excitation wavelength is characteristic of the red edge excitation shift. The observation of REES for NBD-cholesterol incorporated in AOT reverse micelles implies that the NBD group is located in a motionally restricted environment. Unlike the NBD group of NBD-PE which is located at the reverse micellar interface,[15] the NBD group in NBD-cholesterol is located in the deep acyl chain region of the reverse micelle (see above). Observation of REES for a fluorophore in this region therefore suggests that this region of the reverse micelle can offer restriction to the rotation of solvent dipoles around the excited-state fluorophore. These results assume significance in the context of recent reports of slow (∼nanoseconds) water relaxation in reverse micelles.[57,58]

It is known that the dynamics of liquids in confined spaces is different from that of their bulk counterparts[10,59,60] and this constitutes one of the main reasons for the popularity that reverse micelles enjoy as a model system in studies of water dynamics. The highly structured yet heterogeneous water molecules in reverse micelles represent interesting models for water molecules present in biological systems such as membranes which are more difficult to analyze experimentally. The properties of water in reverse micelles of AOT at low w_o values are rather different from those of bulk water.[7−9] Even at higher water content ($w_o = 50$), the apparent microviscosity is 6−9 times greater than that of free aqueous solutions.[61] Three types of water populations (pools) coexist in reverse micelles. These are bound water, trapped water, and free water.[8,9,57] The crucial parameter is the [water]/[surfactant] molar ratio which determines the relative proportions of these three types of water pools. The trapped water pool is characterized by the fact that this population of water molecules does not hydrogen bond to other water molecules[9,11] and is most likely to solvate probe molecules such as NBD-cholesterol that are deeper in the acyl chain region of the reverse micelle.

The magnitude of REES obtained as a function of w_o is shown in Figure 5b. Interestingly, the extent of REES increases with increasing water-to-surfactant ratio. Thus, REES increases from 6 to 11 nm when w_o is increased from 0 to 25. This indicates that addition of water to the reverse micellar system leads to an increase in the overall motional restriction experienced by the reorienting solvent molecules in the region of localization of the NBD group. This is surprising since water relaxation rates in reverse micelles have been shown to become faster with an increase in w_o.[62] This increase in reorientation rate is reflected in reduced REES for probes at the reverse micellar interface[15,63] and water pool.[64] In contrast to these reports, our results show an increase in the motional restriction experienced by reorienting solvent molecules around NBD-cholesterol with increased water-to-surfactant molar ratio. This difference could possibly be due to the deeper location of the NBD group in the reverse micellar assembly implying that the rate of solvent relaxation (reorientation) varies with probe location. We have earlier shown such depth-dependent solvent relaxation in NBD-labeled lipid probes[23] and anthroyloxy fatty acid probes[21] bound to membranes.

Fluorescence Polarization and Lifetime of NBD-Cholesterol with Varying Hydration and Wavelength. The steady-

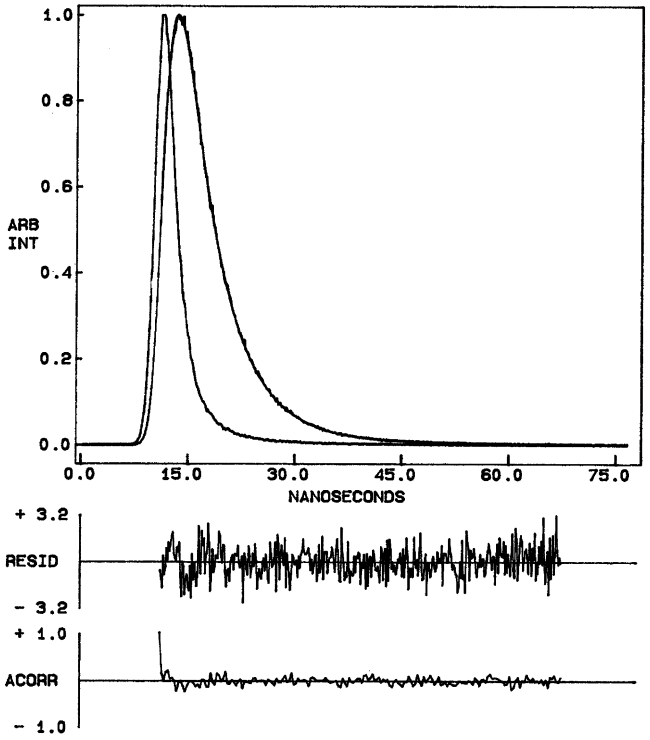

Figure 7. Time-resolved fluorescence intensity decay of NBD-cholesterol in AOT reverse micelles at $w_o = 10$. Excitation wavelength was at 465 nm and emission was monitored at 513 nm. The sharp peak on the left is the lamp profile. The relatively broad peak on the right is the decay profile, fitted to a biexponential function. The two lower plots show the weighted residuals and the autocorrelation function of the weighted residuals. All other conditions are as in Figure 4. See Experimental Section for other details.

state polarization of NBD-cholesterol in AOT reverse micelles as a function of increasing amounts of water is shown in Figure 6a. As shown in the figure, fluorescence polarization of NBD-cholesterol decreases with increasing w_o which implies that there is a decrease in rotational restriction experienced by the NBD group with increasing hydration (assuming that the change in fluorescence lifetime is not significant; see later). Fluorescence polarization depends on the excitation wavelength in viscous solutions or otherwise motionally restricted media.[28] Figure 6b shows the fluorescence polarization of NBD-cholesterol in AOT reverse micelles of various w_o plotted as a function of excitation wavelength. The considerable increase in fluorescence polarization in all cases as the excitation wavelength is shifted toward the red edge reinforces our earlier conclusion that the NBD group is in a motionally restricted environment in the reverse micelle.

Since fluorescence lifetime serves a sensitive indicator of the local environment around a given fluorophore[65] and is sensitive to excited-state interactions, differential extents of solvent relaxations around a given fluorophore could be expected to give rise to differences in its lifetime. In addition, it is well known that fluorescence lifetime of the NBD group is sensitive to the environment in which it is placed and is reduced in the presence of water.[54,55,66] A typical decay profile of NBD-cholesterol in AOT reverse micelles with its biexponential fitting and the various statistical parameters used to check the goodness of the fit is shown in Figure 7. The fluorescence lifetimes of NBD-cholesterol in AOT reverse micelles obtained as a function of w_o are shown in Table 1. As seen from the table, all fluorescence decays could be fitted well with a biexponential function. We chose to use the mean fluorescence lifetime as an important parameter for describing the behavior of NBD-

TABLE 1: Lifetimes of NBD-cholesterol in AOT Reverse Micelles as a Function of w_o [a]

[water]/[surfactant] molar ratio[b] (w_o)	α_1	τ_1 (ns)	α_2	τ_2 (ns)	χ^2
0	0.56	6.05	0.44	3.68	1.13
2	0.39	6.03	0.61	3.42	1.16
4	0.65	5.15	0.35	2.53	1.18
10	0.38	5.57	0.62	3.11	1.08
15	0.45	5.31	0.55	2.77	1.12
20	0.38	5.52	0.62	2.94	1.34
25	0.34	5.77	0.66	3.10	1.36

[a] The excitation wavelength was 465 nm; emission was monitored at 513 nm. [b] The ratio of NBD-cholesterol to AOT was 1:6250 (mol/mol).

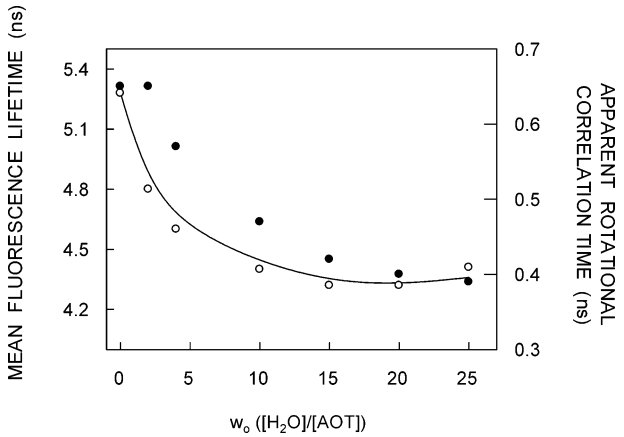

Figure 8. Effect of increasing amounts of water on mean fluorescence lifetime (○) of NBD-cholesterol in AOT reverse micelles. The excitation wavelength used was 465 nm and emission wavelength was set at 513 nm. Mean fluorescence lifetimes were calculated from Table 1 using eq 3. All other conditions are as in Figure 4. See Experimental Section for other details. The apparent rotational correlation times (●) of NBD-cholesterol in AOT reverse micelles are also shown. The apparent rotational correlation times are calculated using eq 4 (see text for details).

cholesterol bound to AOT reverse micelles since it is independent of the number of exponentials used to fit the time-resolved fluorescence decay. The mean fluorescence lifetimes of NBD-cholesterol in AOT reverse micelles were calculated using eq 3 and are plotted as a function of w_o in Figure 8. The increased polarity around the NBD group of NBD-cholesterol in AOT reverse micelles with increasing w_o is reflected in the decrease in the mean lifetime of NBD-cholesterol with increase in the reverse micellar water content. Interestingly, the fluorescence lifetime decreases sharply when small amounts of water are added (up to $w_o = 10$), followed by a plateau when w_o is increased up to 25.

To ensure that the observed change in steady-state polarization of NBD-cholesterol as a function of w_o (see Figure 6a) is not due to any change in lifetime with increasing w_o (Figure 8), the apparent (average) rotational correlation times for NBD-cholesterol in AOT reverse micelles with increasing w_o were calculated using Perrin's equation:[43]

$$\tau_c = \frac{\langle\tau\rangle r}{r_o - r} \tag{4}$$

where r_o is the limiting anisotropy of NBD, r is the steady-state anisotropy (derived from the polarization values using $r = 2P/(3 - P)$), and $\langle\tau\rangle$ is the mean fluorescence lifetime as calculated from eq 3. Although Perrin's equation is not strictly applicable to this system, it is assumed that this equation will

TABLE 2: Lifetimes of NBD-Cholesterol as a Function of Excitation Wavelength[a]

excitation wavelength (nm)	α_1	τ_1 (ns)	α_2	τ_2 (ns)	χ^2
		(a) $w_o = 0$			
465	0.56	6.05	0.44	3.68	1.13
475	0.73	5.46	0.27	2.55	1.35
485	0.36	6.08	0.64	3.56	1.37
490	0.56	5.30	0.44	2.43	1.30
495	0.57	4.92	0.43	1.83	1.23
		(b) $w_o = 2$			
465	0.39	6.03	0.61	3.42	1.16
475	0.61	5.02	0.39	2.12	1.30
485	0.41	5.57	0.59	2.67	1.20
490	0.46	5.00	0.54	2.40	1.16
495	0.49	4.20	0.51	1.53	1.44
		(c) $w_o = 25$			
465	0.34	5.77	0.66	3.10	1.36
475	0.59	4.73	0.41	2.03	1.30
485	0.37	5.04	0.63	2.01	1.29
490	0.24	4.46	0.76	1.16	1.41
495	0.15	4.40	0.85	1.03	1.46

[a] Emission wavelength 513 nm.

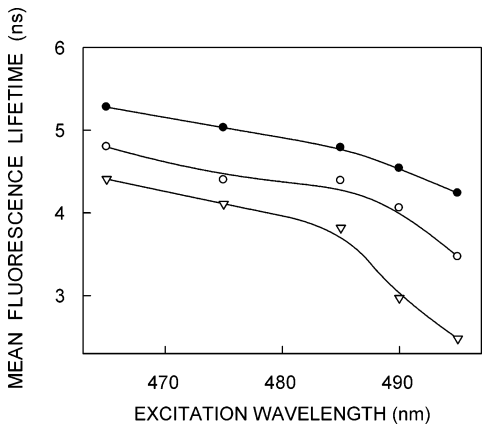

Figure 9. Mean fluorescence lifetime of NBD-cholesterol in AOT reverse micelles corresponding to $w_o = 0$ (●), 2 (○), and 25 (▽) as a function of excitation wavelength. Emission wavelength was kept constant at 513 nm. Mean fluorescence lifetimes were calculated from Table 2 using eq 3. All other conditions are as in Figure 4. See Experimental Section for other details.

apply to a first approximation, especially because we have used mean fluorescence lifetimes for the analysis of multiple component lifetimes. The values of the apparent rotational correlation times, calculated this way using a value of r_o of 0.354,[25] are shown in Figure 8. The overall change in rotational correlation times of NBD-cholesterol with increasing w_o shows that the observed change in polarization values (Figure 6a) were not due to any lifetime-induced artifacts and reinforces our earlier conclusion that there is a decrease in rotational restriction experienced by the NBD group with increasing hydration.

Table 2 shows the lifetimes of NBD-cholesterol in reverse micelles of AOT as a function of excitation wavelength, keeping the emission wavelength constant at 513 nm. All fluorescence decays could be fitted well with a biexponential function. The mean fluorescence lifetimes were calculated using eq 3 and are plotted as a function of excitation wavelength in Figure 9. As shown in this figure, there is a decrease in the mean lifetimes of NBD-cholesterol (especially toward longer wavelengths) with increasing excitation wavelength from 465 to 495 nm when incorporated in reverse micelles of a range of [water]/[surfactant] molar ratio (w_o). Such a marked shortening of mean fluorescence lifetimes at the red edge of the absorption band is indicative of slow solvent reorientation around the excited-state fluorophore.[28] The extent of decrease in mean fluorescence lifetime with excitation wavelength is more pronounced at higher values of w_o which also corresponds to increased REES (see Figure 5b).

Discussion

Reverse micellar systems represent attractive models for biomembranes since they mimic several important and essential features of biological membranes although lacking much of the complexity associated with them. In particular, reverse micelles offer the unique advantage of monitoring the dynamics of bound molecules with varying degrees of hydration by varying the [water]/[surfactant] molar ratio (w_o), which is difficult to achieve with complex systems such as membranes. We have earlier reported using the interfacially located NBD-PE that wavelength-selective fluorescence in general, and REES in particular, can be used as a sensitive tool to probe the changing dynamic hydration profile at the reverse micellar interfacial region.[15]

The ability of a fluorophore incorporated in a reverse micellar assembly to exhibit red edge effects will depend on several factors such as its polarity, as well as the effective polarity of its immediate environment, and its fluorescence characteristics (e.g., lifetime). Since all these properties of a probe are a function of its location in the reverse micelle, the extent of REES would depend on its location in the reverse micelle. The choice of a suitable probe is of considerable importance in wavelength-selective fluorescence studies of organized molecular assemblies.[17,21,23] NBD-labeled probes are appropriate for such studies since the dipole moment of the NBD group changes by ~4 D upon excitation,[67] an important criterion for a fluorophore to exhibit REES effects.[28,31] Further, the NBD group possesses some of the most desirable properties for serving as an excellent probe for spectroscopic applications.[40,41] It is very weakly fluorescent in water and upon transfer to hydrophobic media, it fluoresces brightly in the visible range and shows a large degree of environmental sensitivity.[39,54,55,67,68] This large degree of environmental sensitivity of NBD fluorescence can prove to be very useful in probing different types of reverse micellar organizations formed under various conditions of [water]/[surfactant] molar ratio. For example, the observation that NBD lifetimes are shortened in the presence of water[54,55,66] could prove to be an effective tool in exploring water dynamics in reverse micelles with varying degrees of [water]/[surfactant] molar ratio.

We have previously shown, using NBD and anthroyloxy-labeled membrane probes, that depth-dependent solvent relaxation, as monitored by the wavelength-selective fluorescence approach, can be used as a "dipstick" in membranes.[21,23] In this paper, we have reported depth-dependent solvent relaxation effects in the reverse micellar assembly, using the deeply embedded probe NBD-cholesterol. The use of this probe has allowed us to obtain a solvent relaxation profile of reverse micelles at different extents of hydration. Our results show that with increasing hydration, the NBD group of NBD-cholesterol experiences increased polarity as evidenced by the decrease in fluorescence lifetime and other fluorescence parameters such as fluorescence intensity. Surprisingly, the extent of REES of NBD-cholesterol in reverse micelles increases with increasing water-to-surfactant ratio implying that increasing w_o leads to an increase in the overall motional restriction experienced by the reorienting solvent molecules. We attribute this result to the deeper location of the NBD group in the reverse micellar assembly and conclude that the rate of solvent relaxation (reorientation) varies with probe location.

Acknowledgment. This work was supported by the Council of Scientific and Industrial Research, Government of India. We thank Y.S.S.V. Prasad and G.G. Kingi for technical help. We would like to express our thanks and appreciation to Shanti Kalipatnapu, H. Raghuraman, and Thomas Pucadyil for reading the manuscript critically and for providing useful comments. D.A.K. thanks the Council of Scientific and Industrial Research for the award of a Senior Research Fellowship.

References and Notes

(1) Luisi, P. L.; Magid, L. J. *CRC Crit. Rev. Biochem.* **1986**, *20*, 409.
(2) Luisi, P. L.; Giomini, M.; Pileni, M. P.; Robinson, B. H. *Biochim. Biophys. Acta* **1988**, *947*, 209.
(3) Tanford, C. *Science* **1978**, *200*, 1012.
(4) Israelachvili, J. N.; Marcelja, S.; Horn, R. G. *Q. Rev. Biophys.* **1980**, *13*, 121.
(5) Tanford, C. *The Hydrophobic Effect: Formation of Micelles and Biological Membranes*; Wiley-Interscience: New York, 1980.
(6) Tanford, C. *Biochem. Soc. Trans.* **1987**, *15*, 1S.
(7) Venables, D. S.; Huang, K.; Schmuttenmaer, C. A. *J. Phys. Chem. B* **2001**, *105*, 9132.
(8) Ikushima, Y.; Saito, N.; Arai, M. *J. Colloid Interface Sci.* **1997**, *186*, 254.
(9) Jain, T. K.; Varshney, M.; Maitra, A. *J. Phys. Chem.* **1989**, *93*, 7409.
(10) Brubach, J.-B.; Mermet, A.; Filabozzi, A.; Gerschel, A.; Lairez, D.; Krafft, M. P.; Roy, P. *J. Phys. Chem. B* **2001**, *105*, 430.
(11) Faeder, J.; Ladanyi, B. M. *J. Phys. Chem. B* **2000**, *104*, 1033.
(12) Eastoe, J.; Young, W. K.; Robinson, B. H.; Steytier, D. C. *J. Chem. Soc. Faraday Trans.* **1990**, *86*, 2883.
(13) Melo, E. P.; Aires-Barros, M. R.; Cabral, J. M. S. *Biotechnol. Annu. Rev.* **2001**, *7*, 87.
(14) Behera, G. B.; Mishra, B. K.; Behera, P. K.; Panda, M. *Adv. Colloid Interface Sci.* **1999**, *82*, 1.
(15) Chattopadhyay, A.; Mukherjee, S.; Raghuraman, H. *J. Phys. Chem. B* **2002**, *106*, 13002.
(16) Raghuraman, H.; Chattopadhyay, A. *Langmuir* **2003**, *19*, 10332.
(17) Chattopadhyay, A.; Mukherjee, S. *Biochemistry* **1993**, *32*, 3804.
(18) Mukherjee, S.; Chattopadhyay, A. *Biochemistry* **1994**, *33*, 5089.
(19) Rawat, S. S.; Mukherjee, S.; Chattopadhyay, A. *J. Phys. Chem. B* **1997**, *101*, 1922.
(20) Ghosh, A. K.; Rukmini, R.; Chattopadhyay, A. *Biochemistry* **1997**, *36*, 14291.
(21) Chattopadhyay, A.; Mukherjee, S. *Langmuir* **1999**, *15*, 2142.
(22) Rawat, S. S.; Chattopadhyay, A. *J. Fluoresc.* **1999**, *9*, 233.
(23) Chattopadhyay, A.; Mukherjee, S. *J. Phys. Chem. B* **1999**, *103*, 8180.
(24) Kelkar, D. A.; Ghosh, A.; Chattopadhyay, A. *J. Fluoresc.* **2003**, *13*, 459.
(25) Mukherjee, S.; Raghuraman, H.; Dasgupta, S.; Chattopadhyay, A. *Chem. Phys. Lipids* **2004**, *127*, 91.
(26) Raghuraman, H.; Pradhan, S. K.; Chattopadhyay, A. *J. Phys. Chem. B* **2004**, *108*, 2489.
(27) Raghuraman, H.; Chattopadhyay, A. *Eur. Biophys. J.* **2004** (in press).
(28) Mukherjee, S.; Chattopadhyay, A. *J. Fluoresc.* **1995**, *5*, 237.
(29) Chattopadhyay, A. In *Fluorescence Spectroscopy, Imaging and Probes*; Kraayenhof, R., Visser, A. J. W. G., Gerritsen, H. C., Eds.; Springer-Verlag: Heidelberg, Germany 2002; pp 211−224.
(30) Raghuraman, H.; Kelkar, D. A.; Chattopadhyay, A. *Proc. Ind. Natl. Sci. Acad. A* **2003**, *69*, 25.
(31) Chattopadhyay, A. *Chem. Phys. Lipids* **2003**, *122*, 3.
(32) Demchenko, A. P. *Trends Biochem. Sci.* **1988**, *13*, 374.
(33) Demchenko, A. P. *Luminescence* **2002**, *17*, 19.
(34) Galley, W. C.; Purkey, R. M. *Proc. Natl. Acad. Sci. U.S.A.* **1970**, *67*, 1116.
(35) Lakowicz, J. R.; Keating-Nakamoto, S. *Biochemistry* **1984**, *23*, 3013.
(36) Israelachvili, J.; Wennerstörm, H. *Nature* **1996**, *379*, 219.
(37) Chattopadhyay, A. *Chem. Phys. Lipids* **1990**, *53*, 1.
(38) Chattopadhyay, A.; London, E. *Biochemistry* **1987**, *26*, 39.
(39) Chattopadhyay, A.; London, E. *Biochim. Biophys. Acta* **1988**, *938*, 24.
(40) Mukherjee, S.; Chattopadhyay, A. *Biochemistry* **1996**, *35*, 1311.
(41) Rukmini, R.; Rawat, S. S.; Biswas, S. C.; Chattopadhyay, A. *Biophys. J.* **2001**, *81*, 2122.
(42) Zhou, G.-W.; Li, G.-Z.; Chen, W. J. *Langmuir* **2002**, *18*, 4566.
(43) Lakowicz, J. R. In *Principles of Fluorescence Spectroscopy*; Kluwer-Plenum Press: New York, 1999.
(44) Bevington, P. R. In *Data Reduction and Error Analysis for the Physical Sciences*; McGraw-Hill: New York, 1969.
(45) O'Connor, D. V.; Phillips, D. In *Time-Correlated Single Photon Counting*; Academic Press: London, 1984; pp 180−189.
(46) Lampert, R. A.; Chewter, L. A.; Phillips, D.; O'Connor, D. V.; Roberts, A. J.; Meech, S. R. *Anal. Chem.* **1983**, *55*, 68.
(47) Grinvald, A.; Steinberg, I. Z. *Anal. Biochem.* **1974**, *59*, 583.
(48) Cohen, B.; Huppert, D.; Solntsev, K. M.; Tsfadia, Y.; Nachliel, E.; Gutman, M. *J. Am. Chem. Soc.* **2002**, *124*, 7539.
(49) Mitra, B.; Hammes, G. G. *Biochemistry* **1990**, *29*, 9879.
(50) Wolf, D. E.; Winiski, A. P.; Ting, A. E.; Bocian, K. M.; Pagano, R. E. *Biochemistry* **1992**, *31*, 2865.
(51) Abrams, F. S.; London, E. *Biochemistry* **1993**, *32*, 10826.
(52) Villaín, J.; Prieto, M. *Chem. Phys. Lipids* **1991** *59*, 9.
(53) Abrams, F. S.; Chattopadhyay, A.; London, E. *Biochemistry* **1992**, *31*, 5322.
(54) Lin, S.; Struve, W. S. *Photochem. Photobiol.* **1991**, *54*, 361.
(55) Fery-Forgues, S.; Fayet, J. P.; Lopez, A. *J. Photochem. Photobiol. A* **1993**, *70*, 229.
(56) We have used the term maximum of fluorescence emission in a somewhat wider sense here. In every case, we have monitored the wavelength corresponding to maximum fluorescence intensity, as well as the center of mass of the fluorescence emission. In most cases, both these methods yielded the same wavelength. In cases where minor discrepancies were found, the center of mass of emission has been reported as the fluorescence maximum.
(57) Hazra, P.; Sarkar, N. *Chem. Phys. Lett.* **2001**, *342*, 303.
(58) Bhattacharyya, K.; Bagchi, B. *J. Phys. Chem. A* **2000**, *104*, 10603.
(59) Granick, S. *Science* **1991**, *253*, 1374.
(60) Levinger, N. E. *Science* **2002**, *298*, 1722.
(61) Andrade, S. M.; Costa, S. M. B.; Pansu, R. *Photochem. Photobiol.* **2000**, *71*, 405.
(62) Sarkar, N.; Das, K.; Datta, A.; Das, S.; Bhattacharyya, K. *J. Phys. Chem.* **1996**, *100*, 10523.
(63) Hof, M.; Lianos, P.; Laschewsky, A. *Langmuir* **1997**, *13*, 2181.
(64) Sarkar, M.; Ray, J. G.; Sengupta, P. K. *J. Photochem. Photobiol., A* **1996**, *95*, 157.
(65) Prendergast, F. G. *Curr. Opin. Struct. Biol.* **1991**, *1*, 1054.
(66) Saha, S.; Samanta, A. *J. Phys. Chem. B* **1998**, *102*, 7903.
(67) Mukherjee, S.; Chattopadhyay, A.; Samanta, A.; Soujanya, T. *J. Phys. Chem.* **1994**, *98*, 2809.
(68) Rajarathnam, K.; Hochman, J.; Schindler, M.; Ferguson-Miller, S. *Biochemistry* **1989**, *28*, 3168.